Electronic supplementary information (ESI)

Human Tat-Derived Cyclic Peptide Destabilizes the MALAT1 ENE Triple Helix and Attenuates Expression

Pranotosh Das,[a,b] Shuvam Mandal,[a,b] and Manish Debnath [a,b]*

[a]*Organic and Medicinal Chemistry Division, CSIR-Indian Institute of Chemical Biology, Kolkata 700032, India.*

[b]*Academy of Scientific and Innovative Research (AcSIR), Ghaziabad-201002, India*

Table of Contents

1.0 General Information

N,N'-dimethylformamide (DMF), dichloromethane (DCM), succinic anhydride (SA), O-Benzotriazole-N,N,N',N'-tetramethyluronium hexafluorophosphate (HBTU), piperidine, N, N-diisopropylethylamine (DIPEA), triisopropylsilane (TIPS), and trifluoroacetic acid (TFA) were purchased from Sigma–Aldrich. All Fmoc amino acids and 2-chlorotrityl chloride resins were obtained from Sigma–Aldrich. Hemin, Thioflavin T, 3,3',5,5'-Tetramethylbenzidine (TMB) was procured from Sigma–Aldrich. For all the experiments, buffers required were prepared in the lab containing varying ionic composition and pH. The buffers used is Tris-KCl were used in pH 7. The pH was adjusted by adding HCl. Oligonucleotides were purchased from Integrated DNA Technologies, USA at 50 nM scale and desalted purification grade as single-stranded DNA and used for RNA production, without further purification. Stock solutions of the oligonucleotides with strand concentration of 100 µM were prepared in nuclease-free water and stored at -20 ºC. A549 and HeLa cell lines were procured from ATCC.

2.0 Molecular Docking and Screening

The X-ray determined structure of Metastasis-Associated Lung Adenocarcinoma Transcript 1 (MALAT1) was retrieved from the PDB database (PDB ID: 4PLX). Of the three RNA molecules deposited in the PDB, only the most ordered molecule A was considered. The energy minimized 3d structure of the peptides to be screened were produced using the alphafold 2 server.[1] A blind docking study was performed for the ligand wherein the complete receptor long non-coding RNA was considered for search-space. Screening of the molecules by docking them with the MALAT1 triple using PyRx[2] based on Autodock 4.2 software[3]. The docking scores were used to align the peptides in the decreasing order of binding energy.

3.0 Synthesis of Peptides

For specifically targeting the MALAT1 triplex we developed a linear peptide (LP1) and a conformationally constrained cyclic peptide (CP1). LP1 and CP1 were synthesized by solid phase peptide synthesis using Fmoc chemistry and rest of the peptides in Table 1 were procured commercially from SBiochem, India. Resin and protected amino acids were purchased from TCI and Sigma–Aldrich. Rink Amide resin was used for the synthesis.

Piperidine (20% in DMF) was used for deprotection, and DIC/Oxyma for coupling. The peptides were precipitated and washed with diethyl ether (~20 mL), before collecting the solid and lyophilising from 1:1 MeCN/H_2O + 0.1 v/v% TFA to yield a white solid (~100–120 mg, ~75–80 % crude).

High performance liquid chromatography (HPLC) of CP1 and LP1 were performed to purify the peptides. Identity of peptides were validated by liquid chromatography-mass spectroscopy (LC-MS). Peptides (~30 mg) were dissolved in reaction buffer (20 mM NH_4HCO_3, 5 mM EDTA, pH = 8.0 adj. with NaOH, 12 mL) and MeCN (4 mL). TBMB (50 mM in MeCN, 250 µL) was then added, and the reaction stirred at room temperature for ~1 h, monitoring with LC-MS. The MeCN was removed by using rotary evaporator and the final solution in aqueous phase was subjected to lyophilisation, for the final white dried cyclized product. The mass of the products from the reactions were confirmed through LC-MS.

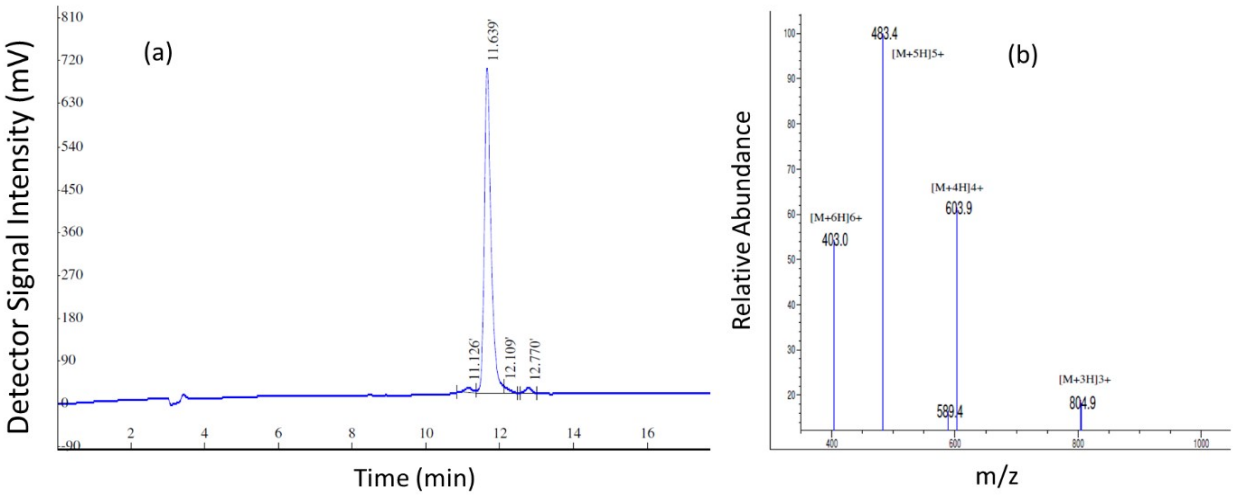

Fig. S1 (a) HPLC results of FITC labelled CP1 peptide. The mobile phase was 0.1% TFA in Acetonitrile and Water and the final ratio v/v is 1:4. The retention time is 11.639 min. (b) LC - MS analysis of the peptide. Molecular weight of the peptide is 2411.82 Da.

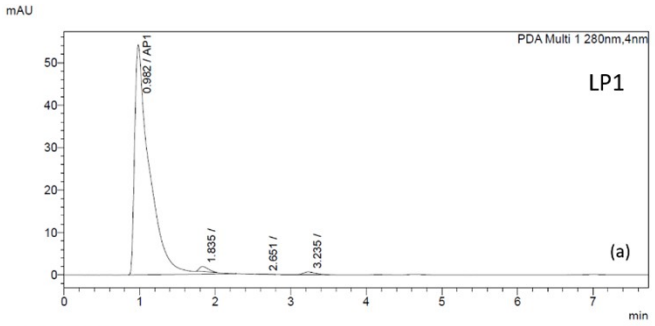

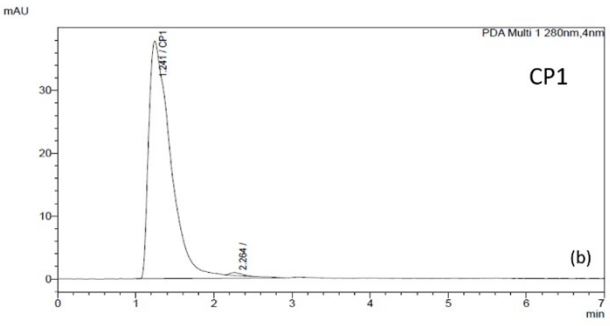

<Peak Table>

PDA Ch1 280nm

Peak#	Ret. Time	Area	Height	Name	Area%
1	0.982	739976	54250	AP1	97.707
2	1.835	9673	1207		1.277
3	2.651	497	62		0.066
4	3.235	7198	653		0.950
Total		757344	56172		100.000

<Peak Table>

PDA Ch1 280nm

Peak#	Ret. Time	Area	Height	Name	Area%
1	1.241	748018	37828	CP1	99.388
2	2.264	4609	452		0.612
Total		752626	38280		100.000

Fig. S2 (a) HPLC of LP1. The mobile phase was 0.1% TFA in Acetonitrile and Water and the final ratio v/v is 1:4; (b) HPLC of CP1. The mobile phase was 0.1% TFA in Acetonitrile and Water and the final ratio v/v is 1:4.

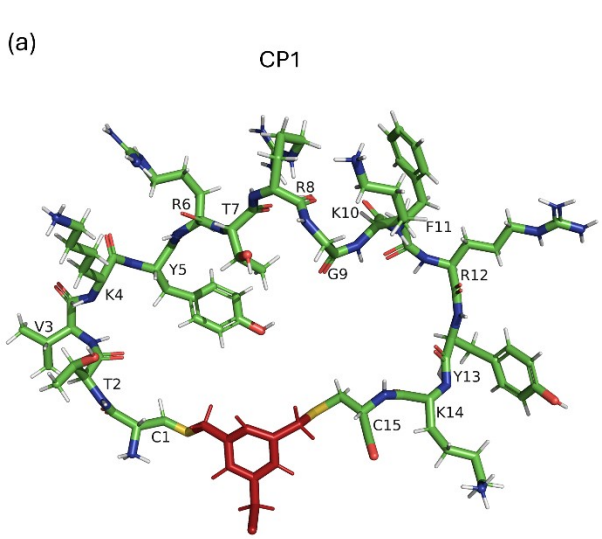

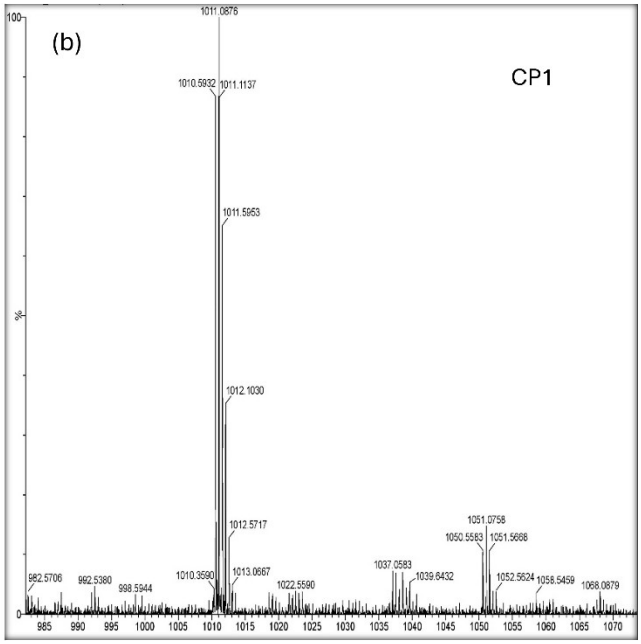

Fig. S3 (a) Structure of CP1; (b) LC-MS analysis of the peptide CP1 (MW 2025 Da).

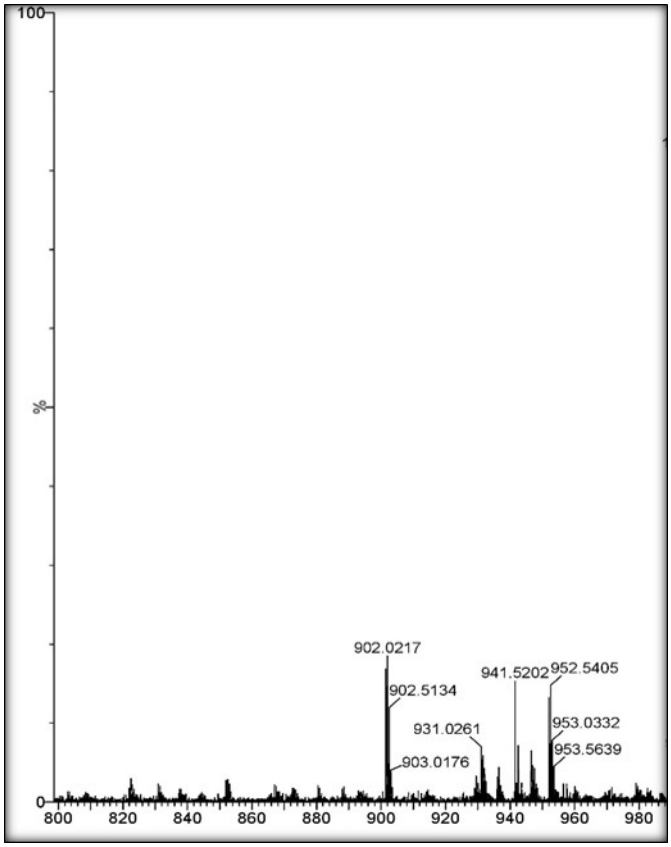

Fig. S4 LC-MS analysis of the peptide LP1 (MW 1907 Da).

4.0 MALAT1 RNA Preparation

All surfaces were cleaned with RNase ZaP prior to handling reagents to avoid RNase contamination. The template and non-template DNA oligos for MALAT1 triple helix and duplex for RNA synthesis were purchased from IDT. The DNA oligos were annealed by heating at 90° C and then slowly cooled to room temperature, to form the double stranded DNA template for RNA synthesis. IVT was performed using the Megascript T7 In-Vitro transcription kit using the DNA templates at 500 ng/µL concentration. The concentration of the RNA was measured using absorbance based nanodrop system. RNA extraction was done for purifying the RNA. Sequence length and purity of the MALAT1 RNA construct was determined using 2.5% agarose gel electrophoresis. The folded triplex was obtained by heating the solutions to 100° C for 5 min and then keeping on ice for 5 min, followed by a slow return to room temperature. All experiments were performed in 10mM Tris, 100mM KCl buffer at pH 7.4. Sequences of the RNA used in this study are listed in Table S1.

Table S1 Sequence of the final RNA utilized for the experiments.

RNA	Sequence (5´-3´)
MALAT1 Duplex RNA	GGAAGGUUUUUCUUUUCCUGAGAAAACAACACGUAUUGUUUUCU CAGGUUUUGCUUUUUGGCCUUUU
MALAT1 Triple Helix RNA	GGAAGGUUUUUCUUUUCCUGAGAAAACAACACUAUUGUUUUCUC AGGUUUUGCUUUUUGGCCUUUUUCUAGCUUAAAAAAAAAAAAAG CAAAA

5.0 Circular Dichroism (CD) Spectroscopy

CD spectra were recorded in a JASCO spectropolarimeter equipped with a thermoelectrically controlled cell holder and a cuvette with a path length of 1 cm. CD spectra for the triplex and control duplex (both 5 µM) were recorded between 200 and 330 nm at 25° C, and the spectrum obtained was the average of three scans. The CD spectra of the LP1 and CP1 were obtained in 1 µM concentration in presence of 10 mM Tris-HCl pH 7 buffer, and the spectrum obtained was the average of three scans. CD spectra of the (5 µM) MALAT1 triple helix and duplex were obtained in presence of 10 mM Tris and 100 mM KCl buffer in pH 7.4. And the titration of the triple helix was performed with the CP1 peptide with increasing concentration

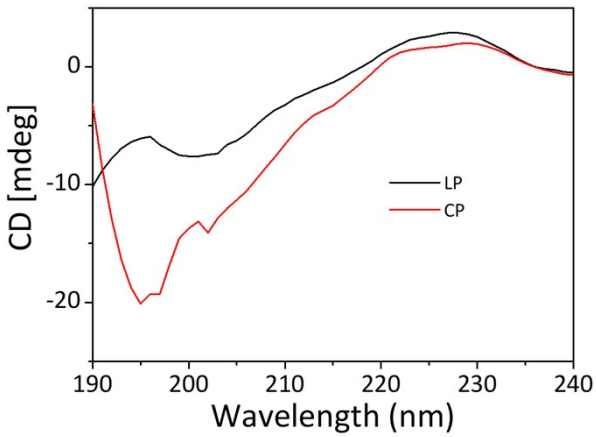

starting from 0.5 eq.

Fig. S5 CD Spectra of linear (LP1) and cyclic (CP1) peptide both at 1 µM concentration.

6.0 Fluorescence Spectroscopy for binding analysis

All fluorescence spectroscopy experiments were performed using Horiba Flurolog spectrofluorometer at 25 °C and a 700 µL quartz cuvette. The excitation wavelength was fixed to 280 nm and emission spectra were collected between 290 and 380 nm with a slit width of 5 nm. The temperature was maintained constantly at 25 °C by an external thermostatic water circulator. To measure peptide-RNA interactions, the peptides (both cyclic and linear) at 1µM concentration were equilibrated in Tris (10 mM)-KCl (200 mM) buffer at pH 7.4. The peptides were excited at 280 nm wavelength and the MALAT1 Triplex and Duplex RNA were added in increasing concentrations and the spectra was recorded, to the point of saturation. The recorded spectral data were used to determine the dissociation constant of the ligands for c-

$$F = F_0 + \frac{(F_{max} - F_0)[DNA]}{K_d + [DNA]}$$

MYC quadruplex using the Hill-1 formula:

where, F is the fluorescence intensity, F_{max} is the maximum fluorescence intensity, F_0 is the fluorescence intensity in the absence of DNA, and K_d is the dissociation constant.

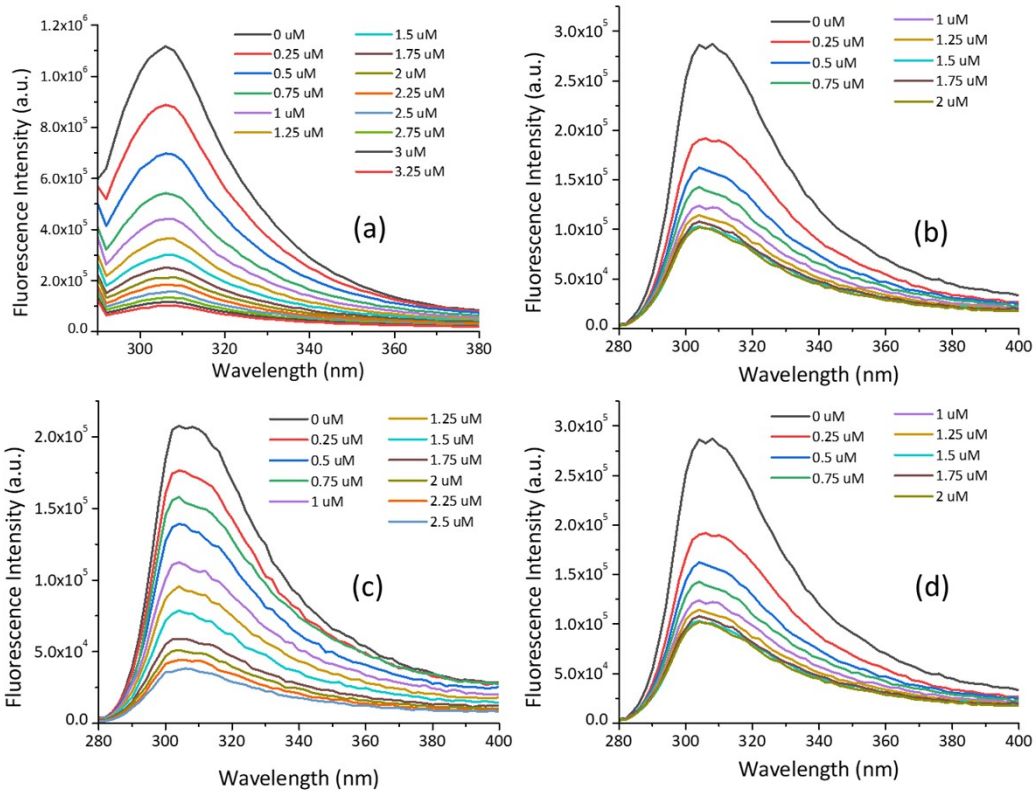

Fig. S6 Emission spectra of CP1 (1 µM) with increasing concentration of (a) MALAT1 triple helix and (b) MALAT1 duplex in presence of 10 mM Tris and 100 mM KCl, pH 7.4; Emission spectra of LP1 (1 µM) with increasing concentration of (c) MALAT1 triple helix and (d) MALAT1 duplex.

7.0 Competitive binding Fluorescence assay

Competitive fluorescence binding experiments were performed using the same instrumental setup and experimental conditions as described above. All measurements were carried out on a Horiba Fluorolog spectrofluorometer at 25 °C using a 700 µL quartz cuvette. The excitation wavelength was fixed at 280 nm, and emission spectra were recorded from 290 to 380 nm with a slit width of 5 nm. Temperature was maintained at 25 °C using an external thermostatic water circulator.

7.1 Competitive binding of peptides with non-triplex sequences

To evaluate the competitive binding of peptides towards different non-triplex nucleic acid structures (Table S2) and genomic RNA, the peptides (1 µM) were first equilibrated in Tris (10 mM)–KCl (200 mM) buffer at pH 7.4. Subsequently, increasing concentrations of pre-folded nucleic acid structures were titrated into the peptide solution. Fluorescence emission spectra were recorded after each addition until saturation was achieved. Changes in intrinsic tryptophan fluorescence intensity were monitored to assess displacement or competitive binding of the peptides toward various nucleic acid topologies.

Table S2 Non-triplex nucleic acid sequences used for fluorescence binding studies

DNA	**Sequence (5´-3´)**
22R	AGGGCGGTGTGGGAAGAGGGAA
c-Kit1	GGGAGGGCGCTGGGAGGAGGG
c-Myc	TGGGGAGGGTGGGGAGGGTGGGGAAGG
ThTC	ACCCCTTTTCCCCAACCCCTTTCCCCA
ThTG	TGAGGGAGGGGTGAGGGAGGGG

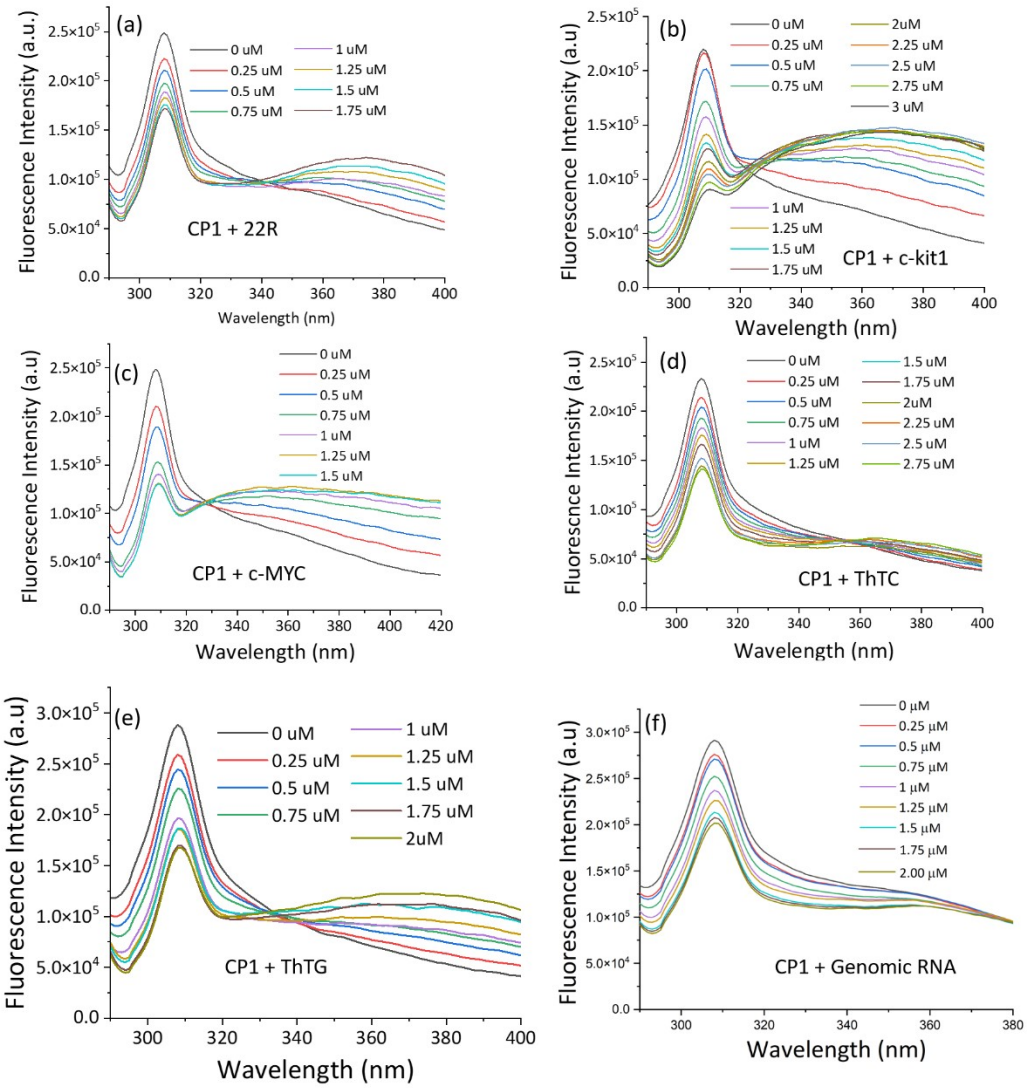

Fig. S7 Emission spectra of CP1 (1 µM) with increasing concentration of nucleic acid structures with increasing concentration of (a) 22R, (b) *c-Kit1* (c) *c-Myc*, (d) Cytosine-rich sequence ThTC, (e) ThTG, and (f) genomic RNA in the presence of Tris (10 mM)-KCl (200 mM) buffer at pH 7.4.

7.2 Competitive binding of MALAT1 Triplex and Duplex RNA with Peptides

In the reciprocal experiment, MALAT1 triplex and duplex RNA structures were used as fluorescent targets. The RNA (fixed concentration) was equilibrated in the same buffer conditions, and peptides containing charged amino acid residues were added incrementally. Upon excitation at 280 nm, emission spectra were recorded after each addition to monitor changes in fluorescence intensity arising from peptide–RNA interactions. The competitive

binding behavior was evaluated based on fluorescence quenching or enhancement relative to the unbound RNA.

For both sets of experiments, the obtained fluorescence data were analyzed using the Hill-1

binding model:

where, F is the fluorescence intensity, F_{max} is the maximum fluorescence intensity, F_0 is the fluorescence intensity in the absence of DNA, and K_d is the dissociation constant.

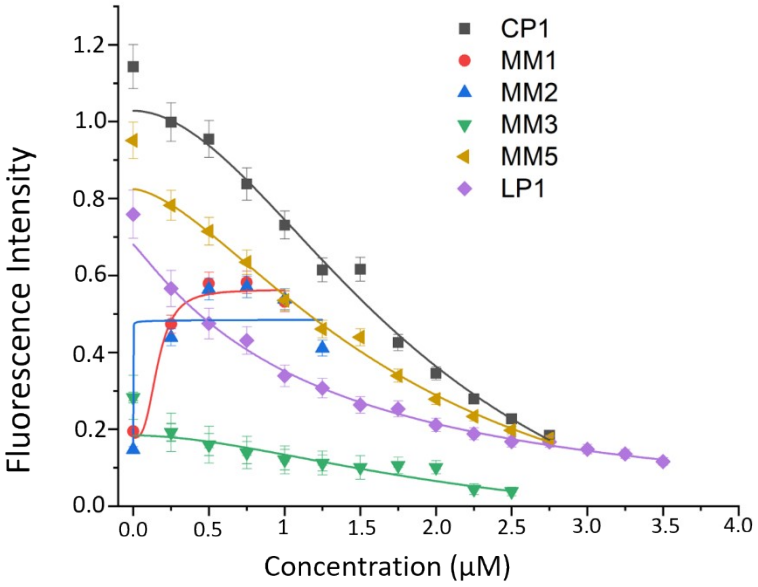

Fig. S8 Change in intrinsic fluorescence from 1 μM positively charged peptides [excitation in 280 nm and emission from 290 to 380 nm] after adding 0-4 μM *MALAT1* triple helix with increasing concentrations of different peptides in buffer conditions 10 mM Tris, 100 mM KCl at pH 7.4. (Error ±SD).

8.0 Isothermal Titration Calorimetry (ITC) studies

Isothermal titration calorimetry experiments were performed on a micro-calorimeter (Malvern, USA). RNA (8 μM) to peptide (100 μM, 6 μL per injection) ratio was taken as 1:10 and the titration was carried out in 10 mM Tris-HCl, 100 mM KCl buffer (pH 7.4) at 25 ˚C. Final analysis of the data was carried out using Originpro 8.0 (OriginLab Corp.).

9.0 Molecular Dynamics (MD) Simulation

9.1 Structure Preparation

To model the CP1, we employed the ff19SB force field.[4] The linker region, composed of 1,3,5-tris-methylbenzene, was described using standard all-atom types: CA and HA for the aromatic carbons and hydrogens, and CT and HC for the methyl group carbons and hydrogens. The cysteine residues forming the thioether linkage to the linker were assigned the CYX residue type, which correctly represents the bonded sulfur state, utilizing default parameters for its bonded geometry. This modeling approach is justified, despite CYX typically denoting a disulfide bond, because the near-identical electronegativity of sulfur (2.58) and carbon (2.55) on the Pauling scale results in a minimal electronic discrepancy for a C–S bond. The overall charge of the synthetic linker is zero. During the initial structure preparation and minimization phase, a Generalized Born implicit solvent model (igb = 2)[5–7] with a 0.15 M salt concentration[8] modeled via the Debye-Hückel approximation was used for the peptide.

9.2 Docking procedure

To prepare the initial complex for molecular dynamics simulations, a systematic docking and conversion procedure was employed. First, the structure of the cyclic peptide-linker construct was prepared using the Xleap module within AmberTools. Initial docking to the MALAT1 RNA was performed using AutoDock 4.2,[9] from which the top-ranked conformation (Conformation 1), with a binding energy of -1.80 kcal/mol, was selected. However, because the atom type representations used by AutoDock are not directly compatible with the Amber force field, a subsequent refinement step was necessary. We therefore identified the binding site defined by this AutoDock pose and manually docked the original Amber-prepared peptide into this site using PyMOL.[10] We placed the linker away from the RNA, and the peptide was brought close enough for interactions to occur, but without introducing atom clashes.

9.3 Molecular Dynamics Simulations

The molecular dynamics simulations were performed using the AMBER24[11] software package with GPU acceleration.[12] The initial structures were solvated in a truncated octahedral box of TIP3P water molecules, maintaining a minimum solvent buffer of 14 Å in all directions. The system was neutralized with K^+ counterions, with an additional 30 Cl^- ions added to approximate physiological salt concentration, employing TIP3P-specific ion parameters.[13] An energy minimization protocol was first executed: an initial 5,000-step minimization with a 50 kcal mol^{-1} harmonic restraint applied to the peptide and RNA, followed by a second, unrestricted minimization. The system was then gradually heated from 0 to 300 K over 100 ps under NVT conditions, using a 2.0 fs time step and a Langevin thermostat[14] with a collision frequency of 0.2 ps^{-1}, while maintaining 50 kcal mol^{-1} positional restraints on all peptide atoms. These restraints were systematically reduced through three successive 50 ps NVT simulations, concluding with a 100 ps unrestrained equilibration at 300 K. Subsequently, density equilibration was achieved through a 250 ps NPT simulation at 300 K and 1 atm,

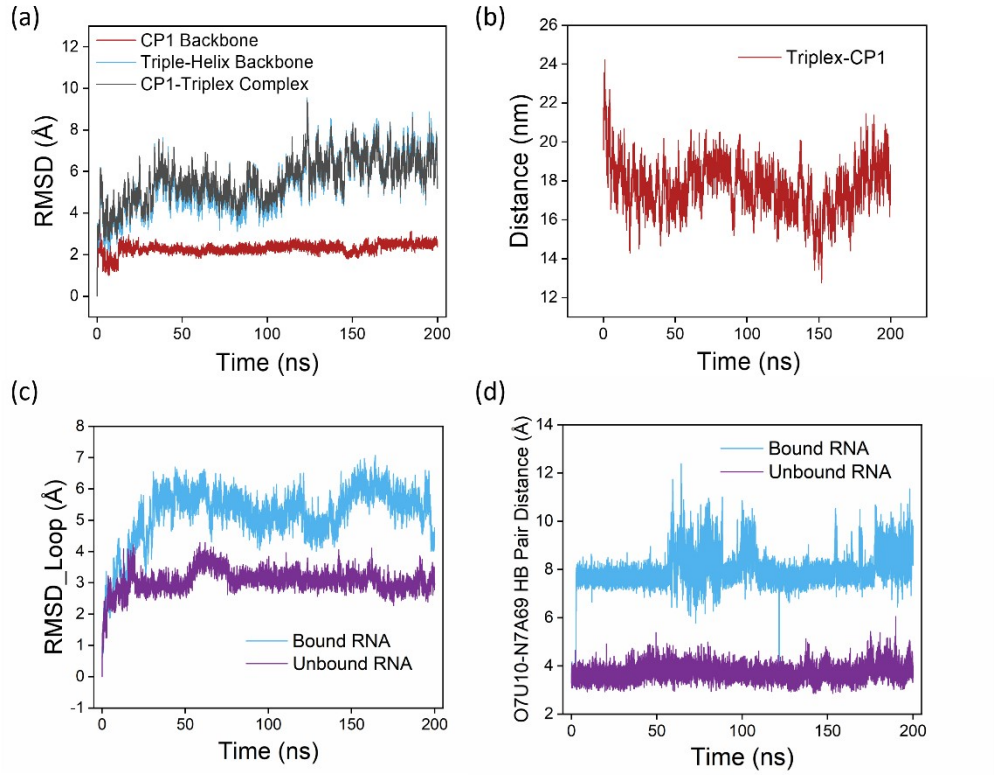

followed by an identical 250 ps simulation without restraints. Finally, production data were collected from a 200 ns unrestrained simulation in the NVT ensemble with 3 such runs. trajectory analysis and visualization carried out using VMD 1.9.3[15] and Pymol[10] for image rendering.

Fig. S9 (a) RMSD plot of CP1 and MALAT1 RNA complex, MALAT1 RNA and the cyclic peptide during 200 ns simulation. Major fluctuations could be observed in MALAT1 RNA as well as the complex. (b) Distance plot between CP1 and MALAT1 RNA. As the simulation progresses, distance between the peptide and RNA decrease and remain unchanged over the time, which indicate also strong binding of the peptide with the RNA. (c) RMSD Plot of the Loop region of unbound MALAT1 RNA and CP1-bound MALAT1 RNA. (d) Hoogsteen-Base Pair distance of O7U10-N7A69 of Unbound & Bound MALAT1 RNA.

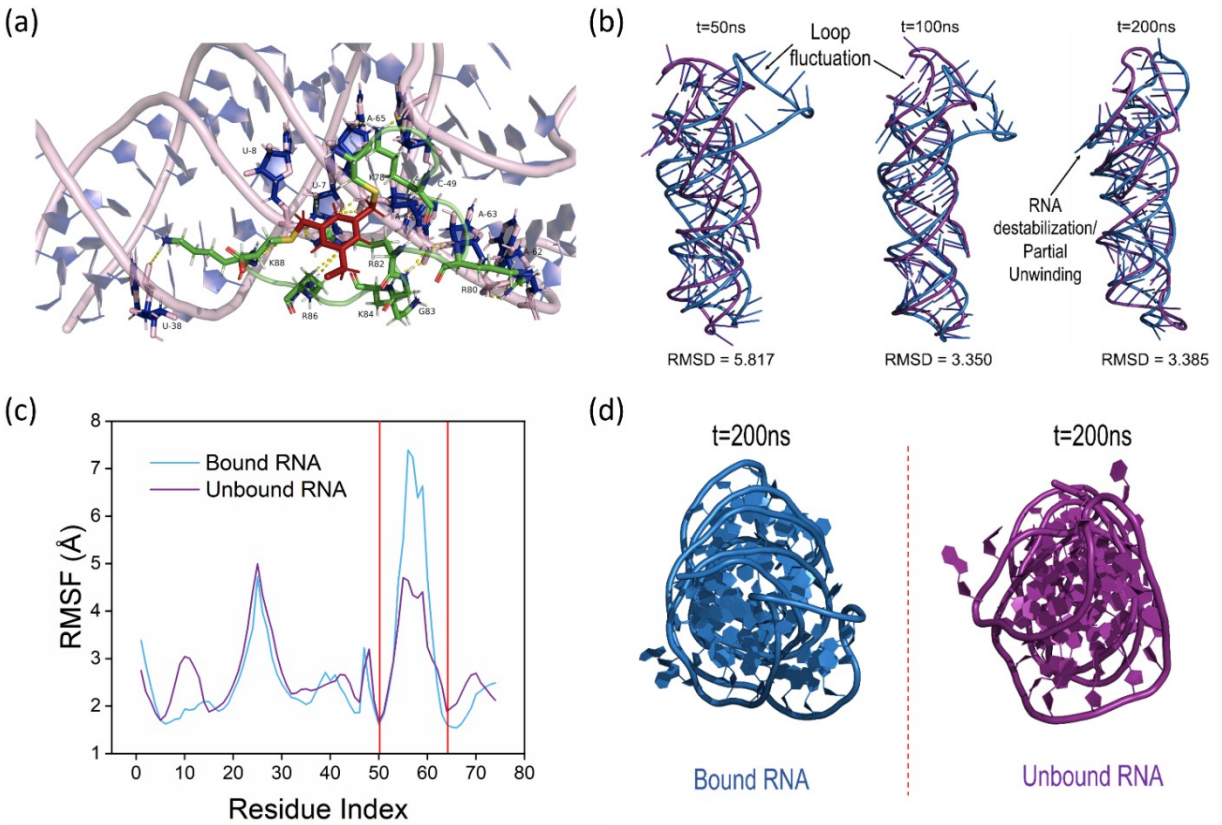

Fig. S10 (a) Visualization of Hydrogen Bond of CP1-MALAT1 RNA after Simulation. (b) Structural Alignment of CP1 bound RNA with unbound RNA at different time point of 200 ns Simulation. (c) Residue-wise Root Mean Square Fluctuation plot of CP1-bound MALAT1 RNA and unbound RNA. Orange coloured bound line indicating Loop region fluctuation in peptide-bound MALAT1 RNA compared to the unbound RNA. (d) Top View of Cyclic Peptide Bound & Unbound MALAT1 RNA after Simulation.

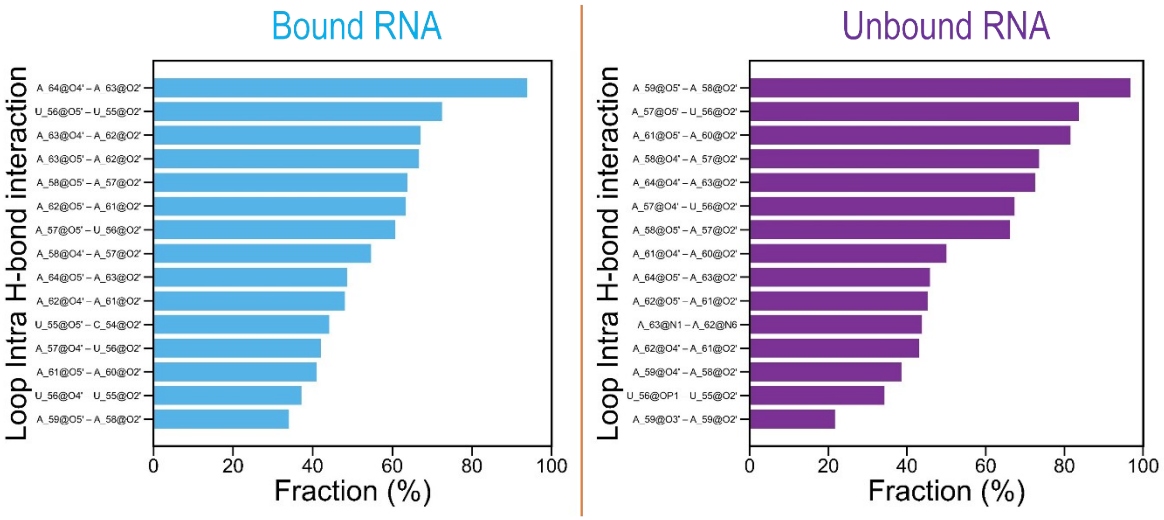

Fig. S11 Loop intra Hydrogen Bond Occupancy Comparison between CP1-bound MALAT1 triplex RNA and Unbound RNA.

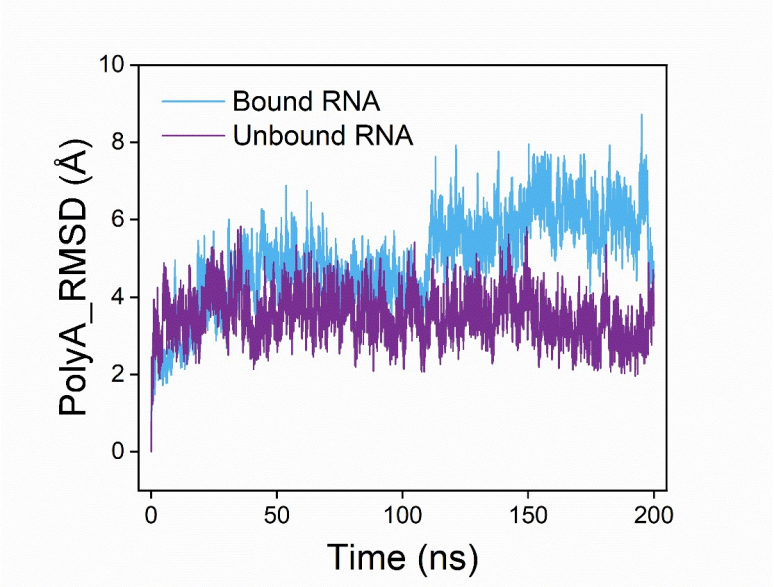

Fig. S12 RMSD Plot of the PolyA tail of unbound MALAT1 RNA and CP1-bound MALAT1 RNA.

10.0 Cell cytotoxicity assay

Cancer Cells (HeLa and A549) and Normal cells (HEK293) were seeded in 96-well plate ($1x10^3$ cells/well) and exposed to various concentrations of LP1 and CP1. XTT (2,3-bis-(2-methoxy-4-nitro-5-sulfophenyl)-2H-tetrazolium-5-carboxanilide) (Thermo Fisher Scientific) solution was prepared by mixing 4 mL (1 mg/mL) in 10 µL of 10 mM PMS (phenazinemethosulfate) (Thermo

Fisher Scientific). After 24 h treatment, 25 µL of XTT/PMS stock solution was added to each well and further incubated for 2 h at 37 °C. Absorbance was measured at 450 nm by an automated microplate reader (Thermo Fisher Scientific). All experiments were performed in parallel and in triplicate, and the IC50 values were derived from the linear regression parameters using GraphPad Prism.

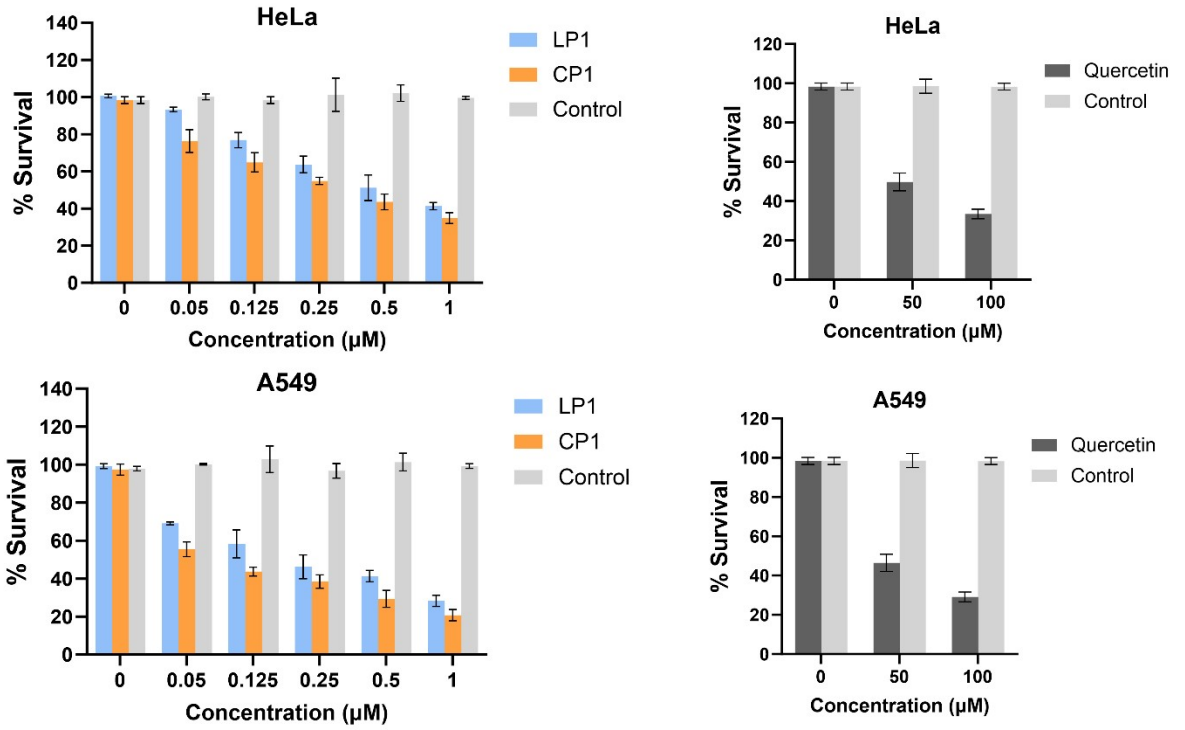

Fig. S13 Evaluation of the cell viability via XTT assay. Cytotoxicity in HeLa cells and A549 (*p = 0,002 < 0.05). Error bars are based on mean ± SD of three experiments. (*p = 0,001 < 0.05 and the related *on the graph, to show if the differences are relevant).

11.0 Intracellular localization of FITC-labeled peptide

For confocal microscopy, 3×10^5 A549 cells were seeded in 35 mm confocal dishes. The cells were washed twice with 1X PBS and incubated with 1000 µL of 0.5 µM FITC-labeled CP1 peptide in OptiMEM for 3 hours at 37 °C with 5% CO_2. Approximately 10 minutes before incubation concludes, two drops of NucRed™ Live 647 ReadyProbes™ Reagent (Thermo Fisher Scientific) per 1 mL was added for effective nuclear staining, ensuring optimal visualization of cell nuclei (as described in the manual). After incubation, the medium was removed, and cells were rinsed twice with 1X PBS before covering them with 1.5 mL of incomplete DMEM. Fluorescence imaging was performed at 37 °C using a Leica SP5-SMD confocal microscope

with a Leica HCX PL Apo CS 63×/1.4NA oil objective lens. NucRed was excited at 641 nm with emission at 661-700 nm, while FITC was excited at 495 nm with emission at 519-525 nm. Sequential image acquisition minimized fluorophore crosstalk, and images were merged and adjusted uniformly using ImageJ software. To quantify the uptake of labelled peptide, region-of-interest (ROI) intensity analysis was performed using ImageJ software. Fluorescence colocalization between CP1-FITC and NucRed was evaluated using scatter plot analysis obtained from confocal microscopy ROIs. The distribution of data points along a positively sloped trend indicated proportional co-distribution of the two fluorescence signals, consistent with the significant positive Pearson correlation coefficient observed.

12.0 Quantitative RT-PCR analysis

Cells were maintained in the 6-well plates in 37 °C, CO2 incubator until 70% confluency was achieved. Further the cells were treated with the CP1 and quercetin (positive control) for 24hr. Next, Extraction of total RNA was performed using Trizol reagent (Invitrogen) following the manufacturer's instructions. The isolated RNA was quantified to determine its concentration and purity. Subsequently, the RNA served as a template for reverse transcription, which was carried out using the cDNA synthesis kit (TAKARA). The reverse transcription process involved incubation at 42 °C for 30 minutes, followed by a denaturation step at 95 °C for 2 minutes, and then cooling to 4 °C to stabilize the cDNA. For quantitative real-time PCR (qRT-PCR), reactions were set up in a Light Cycler® 480 II (Roche) instrument. Each 20 µL reaction mixture contained 10 µL of SYBR Green Master Mix (BioRad), primers at a concentration of 500 nM each (forward and reverse), cDNA at 200 nM, and nuclease-free water to adjust the final volume. The thermal cycling protocol included an initial denaturation at 95 °C for 10 minutes, followed by 40 amplification cycles consisting of denaturation at 95 °C for 15 seconds, annealing and extension at 60 °C for 60 seconds, and a final hold at 37 °C for 2 minutes. The primer sequences used for the qRT-PCR analysis are listed below: MALAT1 (F): 5’-GTTACCAGCCCAAACCTCAA-3’, MALAT1 (R): 5’- CTACATTCCCACCCAGCACT-3’, Krt16 (F): 5’- GACCGGCGGAGATGTGAAC-3’, Krt16 (R): 5’-CTGCTCGTACTGGTCACGC-3’, 18S rRNA (F): 5’-GTAACCCGTTGAACCCCATT-3’, 18S rRNA (R): 5’- CCATCCAATCGGTAGTAGCG-3’. Data represent relative fold change normalized to the control group (baseline = 1.0). Each bar or

point represents the mean ± SD of three independent replicates (n = 3). Statistical significance was determined using a One-Way ANOVA for comparisons against the control group (*p <

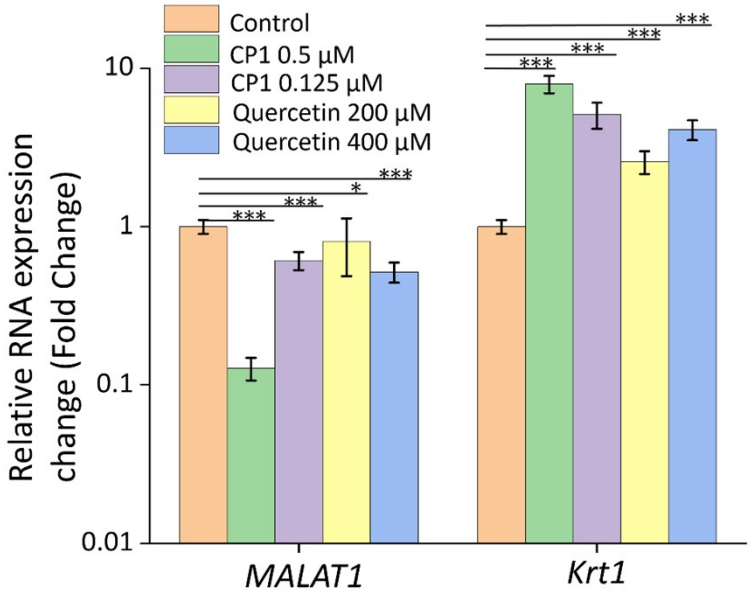

0.05, ***p < 0.001).

Fig. S14. Quantitative real-time PCR showing: fold change in MALAT1 and Krt1 expression levels in A549 cells relative to 18s rRNA as control, upon treatment with the indicated concentrations of the CP1 peptide and quercetin (positive control) for 24 h. RT–qPCR data represent mean ± SD from three independent biological replicates (n = 3), and statistical significance was determined using One-Way ANOVA for comparisons against the control group (*p < 0.05, ***p < 0.001).

13.0 Spheroid culture and Cytotoxicity

The human lung carcinoma cell line A549 was cultured in Dulbecco's Modified Eagle Medium (DMEM) obtained from Sigma–Aldrich, St. Louis, Missouri. The medium was supplemented with 10% fetal bovine serum (FBS) from Invitrogen, Carlsbad, California, along with 2 mM L-glutamine, penicillin at a concentration of 100 U/mL, and streptomycin at 100 U/mL, supplied by Lonza, Basel, Switzerland. Cultures were maintained in a humidified incubator set to 5% carbon dioxide (CO_2) at a temperature of 37°C, ensuring optimal growth conditions for the cells.

13.1 Spheroid Formation and Culture Maintenance

To generate spheroids, A549 cells were first detached from the culture flask using trypsin, an enzymatic agent from Invitrogen. The detached cells were then seeded onto a confocal dish at a density of 3×10^6 cells. The seeding process involved mixing the cells with extracellular matrix (ECM) gel derived from Engelbreth-Holm-Swarm murine sarcoma, obtained from Sigma-Aldrich. The ECM gel was allowed to solidify by incubating the dish at 37°C for 40 minutes, facilitating the formation of a three-dimensional structure. Subsequently, 1 mL of DMEM supplemented with 10% FBS was added to the dish, and the culture was incubated again at 37°C in a humidified environment with 5% CO_2 for 24 hours. The following day, the medium was refreshed with fresh DMEM containing 10% FBS, and the spheroids were cultured for an additional three days. During this period, three-day-old spheroids were treated with specific compounds: 5 µM and 2.5 µM of CP1, and 400 µM of Quercetin, which served as a positive control. These treatments were administered one day prior to assessing cytotoxicity.

13.2 Spheroid Cytotoxicity Assessment

The cytotoxic effects of the treatments were evaluated using confocal laser scanning microscopy. Spheroids were stained with a live/dead viability/cytotoxicity kit designed for mammalian cells, supplied by Thermo Fisher Scientific. This assay enabled the visualization and quantification of cell viability within the spheroids, providing insights into the efficacy of the treatments in inducing cytotoxic effects in the three-dimensional cell culture model.

14.0 Flow cytometry analysis

Annexin V–FITC and propidium iodide (PI) staining are standard methods for distinguishing apoptotic from necrotic cells. Cells were initially harvested through trypsinization after a 24-hour treatment with ligands at increasing concentrations. Following centrifugation at 700 rpm for 5 minutes at 4 °C, the cell pellet was resuspended in 500 µL of 1× binding buffer. Subsequently, 5 µL of Annexin V FITC and 5 µL of PI were added to each sample. After a 5-minute incubation on ice, the samples were immediately analyzed using a fluorescence-activated cell sorting (FACS) instrument, from BD Biosciences (LSRFortessa™). Approximately 10,000 cells per sample were detected, and data analysis was performed using Cell Quest

software. This process allowed quantification of cells in the following stages: viable, early apoptotic, late apoptotic, and necrotic.

The cell cycle distribution was assessed by staining cells with PI, which intercalates into DNA. For this purpose, A549 cells were treated with ligands for 24 hours, then trypsinized and rinsed with phosphate-buffered saline (PBS). The cell pellets were centrifuged and resuspended in 1 mL of PBS, followed by fixation through the dropwise addition of 2 mL of ice-cold 70% ethanol while vortexing vigorously. After fixation, the cells were pelleted again by centrifugation and resuspended in a solution containing 10 µg/mL PI and 10 µg/mL RNase A. The mixture was incubated in the dark at 37 °C for 5 minutes. The stained cells were then analyzed using a flow cytometer, from BD Biosciences (LSRFortessa™), to determine the distribution of cells across different phases of the cell cycle, including G0/G1, S, and G2/M phases.

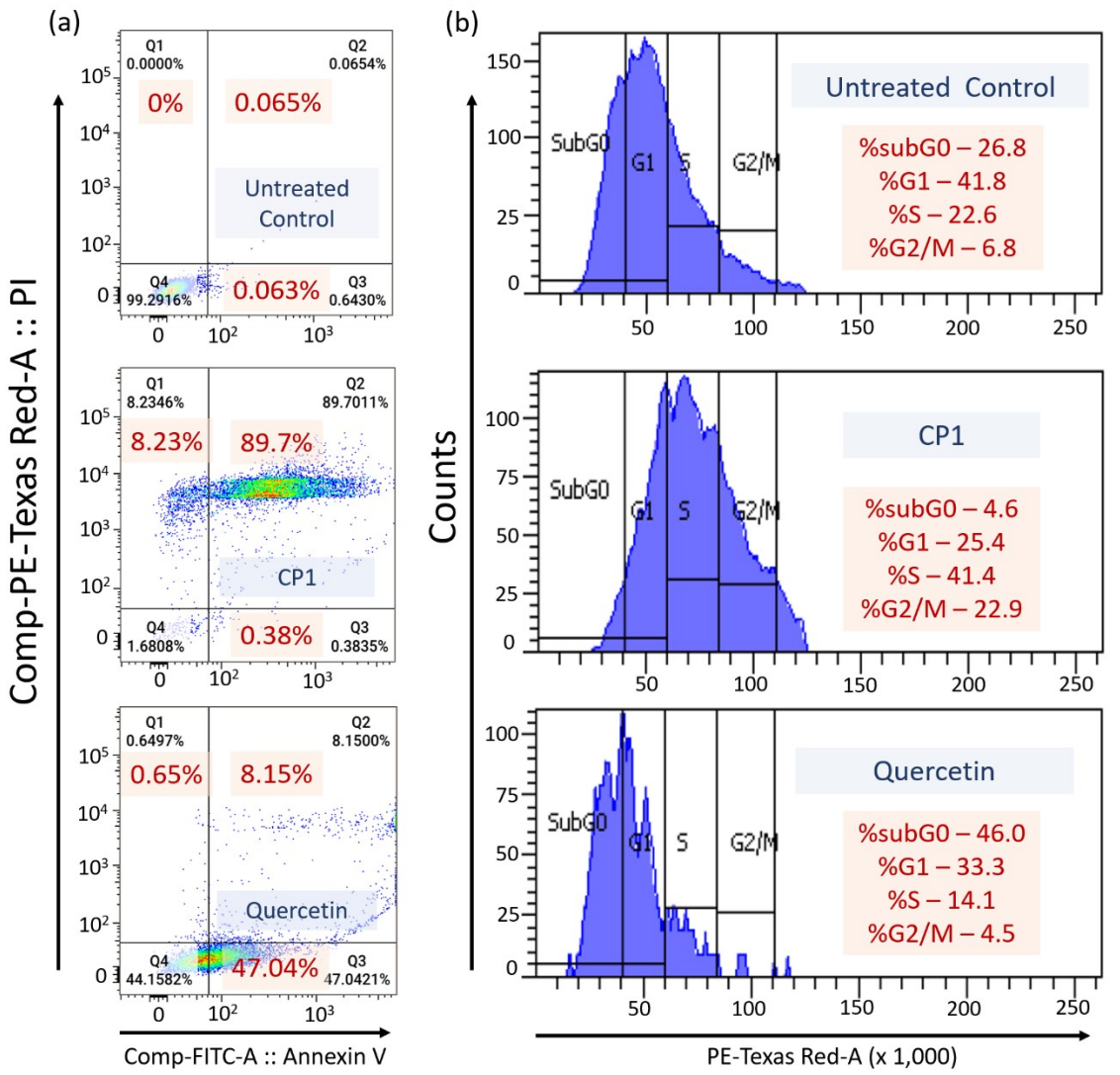

Fig. 15 (a) Flow cytometric analysis of the mode of cancer cell death after treatment with CP1 (0.25 µM), Quercetin (100 µM) in A549 cancer cells; lower left (Q4), lower right (Q3), upper right (Q2) and upper left (Q1) quadrants indicate healthy cancer cells, early, late apoptotic and necrotic cells, respectively. (b) Flow cytometric analysis of cell cycle parameters after incubation of A549 cancer cells with CP1 (0.25 µM) and Quercetin (100 µM) indicating S-phase cell-cycle arrest.

15.0 References

1 J. Jumper, R. Evans, A. Pritzel, T. Green, M. Figurnov, O. Ronneberger, K. Tunyasuvunakool, R. Bates, A. Žídek, A. Potapenko, A. Bridgland, C. Meyer, S. A. A. Kohl, A. J. Ballard, A. Cowie, B. Romera-Paredes, S. Nikolov, R. Jain, J. Adler, T. Back, S. Petersen, D. Reiman, E. Clancy, M. Zielinski, M. Steinegger, M. Pacholska, T. Berghammer, S. Bodenstein,

D. Silver, O. Vinyals, A. W. Senior, K. Kavukcuoglu, P. Kohli and D. Hassabis, *Nat.*, 2021, **596**, 583–589.

2 S. Dallakyan and A. J. Olson, *Methods Mol. Biol.*, 2015, **1263**, 243–250.

3 J. Eberhardt, D. Santos-Martins, A. F. Tillack and S. Forli, *J. Chem. Inf. Model.*, 2021, **61**, 3891–3898.

4 C. Tian, K. Kasavajhala, K. A. A. Belfon, L. Raguette, H. Huang, A. N. Migues, J. Bickel, Y. Wang, J. Pincay, Q. Wu and C. Simmerling, *J. Chem. Theory Comput.*, 2020, **16**, 528–552.

5 A. Onufriev, D. Bashford and D. A. Case, *J. Phys. Chem. B*, 2000, **104**, 3712–3720.

6 A. Onufriev, D. A. Case and D. Bashford, *J. Comput. Chem.*, 2002, **23**, 1297–1304.

7 A. Onufriev, D. Bashford and D. A. Case, *Proteins*, 2004, **55**, 383–394.

8 Application of a pairwise generalized Born model to proteins and nucleic acids: inclusion of salt effects - Rutgers University, https://scholarship.libraries.rutgers.edu/esploro/outputs/journalArticle/Application-of-a-pairwise-generalized-Born/991031716961004646, (accessed March 19, 2026).

9 G. M. Morris, R. Huey, W. Lindstrom, M. F. Sanner, R. K. Belew, D. S. Goodsell and A. J. Olson, *J. Comput. Chem.*, 2009, **30**, 2785–2791.

10 Schrödinger, LLC, 2015.

11 D. A. Case, H. M. Aktulga, K. Belfon, D. S. Cerutti, G. A. Cisneros, V. W. D. Cruzeiro, N. Forouzesh, T. J. Giese, A. W. Götz, H. Gohlke, S. Izadi, K. Kasavajhala, M. C. Kaymak, E. King, T. Kurtzman, T.-S. Lee, P. Li, J. Liu, T. Luchko, R. Luo, M. Manathunga, M. R. Machado, H. M. Nguyen, K. A. O'Hearn, A. V. Onufriev, F. Pan, S. Pantano, R. Qi, A. Rahnamoun, A. Risheh, S. Schott-Verdugo, A. Shajan, J. Swails, J. Wang, H. Wei, X. Wu, Y. Wu, S. Zhang, S. Zhao, Q. Zhu, T. E. I. Cheatham, D. R. Roe, A. Roitberg, C. Simmerling, D. M. York, M. C. Nagan and K. M. Jr. Merz, *J. Chem. Inf. Model.*, 2023, **63**, 6183–6191.

12 A. W. Götz, M. J. Williamson, D. Xu, D. Poole, S. Le Grand and R. C. Walker, *J. Chem. Theory Comput.*, 2012, **8**, 1542–1555.

13 I. S. Joung and T. E. I. Cheatham, *J. Phys. Chem. B*, 2008, **112**, 9020–9041.

14 R. J. Loncharich, B. R. Brooks and R. W. Pastor, *Biopolymers*, 1992, **32**, 523–535.

15 W. Humphrey, A. Dalke and K. Schulten, *J. Mol. Graph.*, 1996, **14**, 33–38.